

Invasion percolation universality class and fractal geometry of magnetic domainsJ. P. Attané,^{1,2,*} M. Tissier,³ A. Marty,^{1,2} and L. Vila^{1,2}¹*Université Joseph Fourier, BP 53, 38041 Grenoble, France*²*INAC, SP2M, CEA Grenoble, 17 avenue des Martyrs, 38054 Grenoble, France*³*Laboratoire de Physique Théorique de la Matière Condensée, 4 Place Jussieu, 75252 Paris Cedex 05, France*

(Received 11 January 2010; revised manuscript received 22 June 2010; published 12 July 2010)

The magnetization reversal process of thin epitaxied FePt/Pt(001) and FePt/MgO(001) layers occurs through rare nucleation events followed by domain-wall propagation. Whereas low-scale observations show that these systems possess very different domain-wall geometries, the structures of the reversed magnetic domains appear to be similar at larger scales: at the beginning of the magnetization reversal, their geometry is that of a fractal percolating cluster. This similarity is analyzed and explained using percolation theory tools and standard domain-growth models, and appears to be an experimental illustration of the universality associated with two-dimensional percolation. We study, in particular, the influence of the demagnetizing field on critical properties and discuss the extent to which these results can be applied to other magnetic thin layers.

DOI: [10.1103/PhysRevB.82.024408](https://doi.org/10.1103/PhysRevB.82.024408)

PACS number(s): 75.60.Ch, 75.60.Jk

In the vicinity of a phase transition, the physical properties depend upon only few elements, as dimensionality and symmetries, and are insensitive to the underlying microscopic properties. Recently, elements of phase-transition theory have been used in order to describe the morphology of a moving interfaces submitted to a random constraint.

The best known applications of phase-transition theory to rough interfaces use 1+1D or 2+1D models. Such models are well adapted to cases where the growth of the interface occurs in a bubblelike geometry: the interface can then be represented by a height function $h(\vec{r})$, with \vec{r} perpendicular to the direction of growth of the interface. In complete absence of disorder, the interface is smooth, i.e., $h(\vec{r})$ is constant. In a disordered environment, the roughness of the interface increases, leading to the development of height fluctuations whose critical behavior is described in the theoretical side by the Kardar-Parisi-Zhang¹ (KPZ) and Edwards-Wilkinson² equations. Those continuous equations and their universality classes have been used to describe magnetic domain-wall (DW) geometries³ as well as many phenomena, ranging from solid surface growth to combustion fronts propagating in sheets of paper.⁴

When the effect of the disorder increases, the roughness will increase until the appearance of dendrites. For strong disorders, the pattern indeed becomes arborescent; consequently the interface cannot be described by an univariate height function, and the 1+1D or 2+1D models of growth become inadequate. For such cases, percolation theory can sometimes provide a description of the interface geometry. In the simple two-dimensional (2D) percolation problem, one considers the probability p for a site to be occupied. At low p , neighboring occupied sites form clusters of finite sizes. When p reaches the percolation threshold p_c , appears a percolating cluster (i.e., a cluster of infinite size). The mean size of the finite clusters is characterized by the correlation length ξ , and the probability for an occupied site to belong to the percolating cluster is given by the order parameter P_∞ (Ref. 6). Both these quantities diverge near P_c : $\xi \propto |p-p_c|^{-\nu}$ and $P_\infty \propto (p-p_c)^{-\beta}$. The critical exponents β and ν do not depend on the type of lattice: they are characteristic of the univer-

sality class associated to bidimensional percolation. Its values have been calculated exactly.⁵

Close to p_c , the geometry of the percolating cluster is fractal: it exhibits self-similarity and scale invariance, which means that small parts of the cluster look similar to the whole cluster. The fractal dimension of the percolating cluster can be related to the critical exponents β and ν

$$D_f = d - \beta/\nu = 91/48 = 1.896,$$

where $d=2$ is the dimension of the lattice.⁶ On a theoretical point of view, this universality class was found to describe correctly the geometry of percolating clusters in the random field Ising model (RFIM) and random bond Ising model (RBIM), when those models are pushed in the limit of strong disorder.^{7,8} This geometry is also those of the percolating cluster in the invasion percolation without trapping (IPWT) problems.⁹ In this model, random values of resistance to fluid invasion are attributed to the cells of a lattice. The fluid is then injected in one cell, with an increasing pressure. The fluid can invade a neighboring cell if the applied pressure overcomes its attributed value of resistance. For a given value of pressure, the fluid will percolate throughout the lattice.

Whatever the model used (simple percolation, RFIM and RBIM at high disorder, or IPWT), the fractal dimension of the percolating cluster is equal to 1.986. In particular, it does not depend on the structure of the lattice.

In a previous paper,¹¹ we showed that FePt/Pt layers possess a square lattice of defects, on which magnetic domain growth can be analyzed as simple percolation in a bond lattice. In this paper, we compare the FePt/Pt system with another kind of magnetic layers, FePt/MgO, which possesses a different microstructure, and thus different domain patterns at low scale, but exhibits similar fractal geometries at large scale, similar to those of a percolating cluster. We show that this phenomenon is a manifestation of universality, being due to the fact that most 2D cells or Ising-type models, taken in the strong disorder limit and without demagnetizing field, can be assimilated to an IPWT process. Using simulations, we finally point out the role of the demagnetizing field,

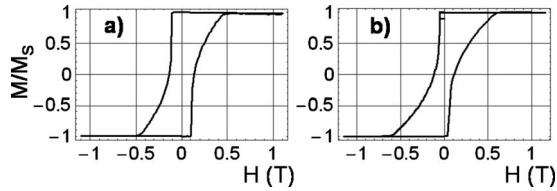


FIG. 1. Hysteresis loops measured in perpendicular field by extraordinary hall effect, in a (a) FePt(32nm)/Pt(40nm)/MgO(001) and a (b) FePt(32nm)/MgO(001) sample. Both loops possess strikingly similar features. In the (b) case, the major loop is followed by a partial reversal of magnetization and a decrease in the magnetic field to zero.

showing that it affects the magnetic domain pattern only at low scales, without modifying the critical properties.

The experimental systems consist of thin FePt layers grown by molecular-beam epitaxy. These layers possess a huge magnetocrystalline anisotropy perpendicular to the sample ($B_a \sim 10$ T), and consequently thin DW and well-defined magnetic domains. In order to obtain different sources of disorder, part of the layers were deposited directly on a Pt(001) substrate, as described in Ref. 10 whereas the other layers were deposited on a MgO(001) substrate. Typical thicknesses of these layers range from 10 to 40 nm. The magnetization reversal of FePt/Pt(001) layers has already been studied in details in Refs. 10 and 11.

As shown in Fig. 1, these two kinds of layers possess similar magnetic properties. The coercive field is about 0.3 T, depending upon the thickness of the sample. The remnant hysteresis loops in perpendicular field [see Fig. 1(b)] allow magnetic imaging by magnetic force microscopy (MFM) at any stage of the magnetization reversal.¹⁰ we emphasize that there is no noticeable change in the magnetization when the applied field is reduced to zero. In this paper, we will focus on the beginning of the magnetization reversal, which in both cases consists of a very sharp drop of the magnetization. The reversal field is applied very slowly ($\sim 10^{-3}$ T s⁻¹), which means that the domain structure results from slow thermo-activated propagation of the domain wall rather than viscous precession-related motion.

We realized several MFM images of samples in remnant magnetic states corresponding to the very beginning of the magnetization reversal. Low-scale images show that the reversed domain is connected in both cases, i.e., it is a single domain. This implies that the reversal occurs through DW propagation from very rare extrinsic nucleation centers. Despite these similitudes, MFM observations show that the low-scale geometries of the domains are very dissimilar. In the FePt/Pt layer [Fig. 2(a)], the epitaxial growth process leads to the formation of structural defects named “microtwins,” inducing a nanostructuring of the layer within a semiperiodic lattice. MFM images demonstrate that the peculiar square geometry of the reversed domain is due to the pinning of the DW on the microtwins. The microtwins formation process as well as the pinning process have been extensively studied in previous papers.^{10–12}

By contrast, FePt/MgO samples present smoothly curved DW [Fig. 2(b)]. Notwithstanding this geometry, which is due to DW energy minimization, the strength of the coercive

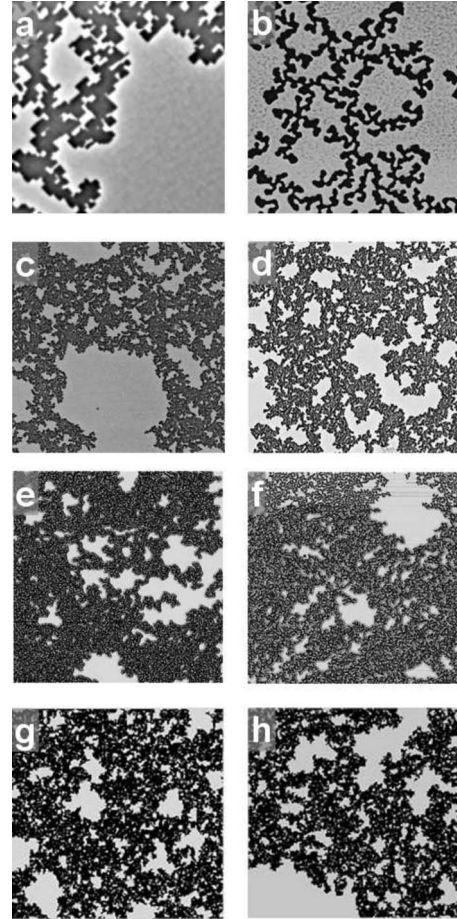


FIG. 2. All these figures correspond to the beginning of the magnetization reversal, the reversed domain appearing in black. (a) $8 \times 8 \mu\text{m}^2$ MFM image of a FePt/Pt sample. The DW is pinned along the microtwins. (b) $8 \times 8 \mu\text{m}^2$ MFM image of a FePt/MgO sample. As there is no microtwin, the DWs are isotropic. (c) and (d): $64 \times 64 \mu\text{m}^2$ MFM images of a FePt/Pt sample. (e) and (f): $64 \times 64 \mu\text{m}^2$ MFM images of a FePt/MgO sample. The domains are fractals, with white parts (unreversed parts) of all sizes. (g) and (h) Simulated geometries of percolating clusters. Although in low-scale (a) and (b) images, domain geometries differ from one kind of sample to another, large-scale images (c), (d), (e), and (f) exhibit for both FePt/Pt and FePt/MgO samples the classical geometry of a percolating cluster shown in (g) and (h). (c), (d), (g), and (h) have already been published in Ref. 11.

field and the fullness of the remanence imply that the DWs are tightly pinned on defects. Structural studies¹³ showed that the strain relaxation process occurs by the creation of a lattice of dislocations at the interface between the MgO substrate and the FePt layer. These defects could interact with DWs through magnetoelastic coupling. TEM observations showed also that there were antiphase boundaries, which can, according to numerical simulations, pin efficiently the DWs in FePt layers. Whichever the source of coercivity in FePt/MgO samples, the pinning defects are microscopically very different from the microtwins, thus generating isotropic DWs geometries instead of square patterns.

Whereas low-scale MFM images ($\sim 1\text{--}8 \mu\text{m}$) show distinct domain geometries in FePt/Pt and FePt/MgO samples,

large images ($\sim 60\text{--}120\ \mu\text{m}$) reveal similar domain structures [Figs. 2(c) and 2(d)]. In both kind of layers and regardless of the thickness of the sample, the structure of the reversed domain is fractal, i.e., there are unreversed (white) part of the sample of all sizes: one can easily find zones larger than $120 \times 120\ \mu\text{m}^2$ (maximal scanning size of our MFM) where there is no reversed domain. Note that, as such images are worthless in studying the reversed domain geometry, we retained only images where the reversed domain cross the four hedges of the image.

We measured the fractal dimension of the reversed domain in several FePt/MgO films, using a box-counting method.¹⁴ Each image is covered by a sequence of grids of descending sizes. For each size of grid are recorded: the number of square boxes intersected by the reversed domain, N , and the side length of the squares, a . The regression slope D of the straight line formed by plotting $\ln(N)$ against $\ln(1/a)$ gives the fractal dimension of the reversed domain. We obtain an average value over 25 MFM images of $D_f = 1.88 \pm 0.02$, very close to the theoretical value of $91/48 \sim 1.896$ of a percolating cluster. Furthermore, there is an excellent qualitative agreement between the geometries of simulated percolating clusters and experimental images [see Figs. 2(g) and 2(h)].

In a previous paper,¹¹ this fractal geometry has been also observed in FePt/Pt layers, and it was shown that the geometry of the reversed domain was analogous to those of a percolating cluster near the percolation threshold, the experimentally observed fractal dimension of the domain being $D_f \sim 1.88$. This geometry was analyzed on the basis of a growth model specifically adapted to the microstructure (square lattice of microtwins) of the FePt/Pt layers. Here, the appearance of a similar pattern in FePt/MgO samples shows that this fractal geometry is not limited to the case of microtwins, but is actually much more general. It also implies that this phenomenon should be studied considering more general models than the percolation in a bond lattice described in Ref. 11. In the following, we will consider the models most commonly used to describe magnetization reversal in 2D magnetic layers, in order to check whether they can explain the observed geometries of the reversed domains.

The simplest models used to describe magnetic domain growth are Ising-type models. In Fig. 2(b) (FePt/MgO), the dendritic structure is given by the energy competition between the demagnetizing field (long-range antiferromagnetic interaction) and the domain-wall energy (short-range ferromagnetic interaction). The third important ingredient involved in the growth process is clearly the disorder (for instance the microtwins in FePt/Pt) that pins the domain walls. A minimal model that takes into account all these interactions is the RFIM with dipolar interactions, whose Hamiltonian is

$$H = \sum_{ij} J_{i,j} S_i S_j - \sum_i [h_i + B(t)] S_i, \quad (1)$$

where $J_{i,j}$ describe both the ferromagnetic nearest-neighbor interaction (i.e., the DW energy) and the dipolar (antiferromagnetic) long-range interaction

$$J_{i,j} = \begin{cases} \alpha - J & \text{if } d(i,j) = 1 \\ \frac{\alpha}{d(i,j)^3} & \text{otherwise,} \end{cases} \quad (2)$$

where $d(i,j)$ is the distance between the spins S_i and S_j , h_i is a random static field, given by a Gaussian probability distribution of width Δ , α is a constant quantifying the importance of the dipolar field, and $B(t)$ is the uniform field that drives the domain growth. A spin can be flipped under the condition that it has at least one returned neighbor. Moreover, in order to account for the very slow increase in the external magnetic field, its value is increased only when no more spin can be flipped.

This model has already been considered in a few studies to describe hysteresis properties (see Ref. 15). It introduces the dipolar interactions, which were first used in the simple 2D Ising model by Sampaio *et al.*,¹⁶ within the RFIM at zero temperature used by Ji and Robbins.^{7,8}

Let us consider first a disorder strength much larger than the exchange term and the demagnetizing field. For a given external magnetic field, only a portion of the sites [those for which $h_i + B(t) > 0$] can be flipped. Consequently, the problem boils down to an IPWT problem,⁹ the pressure and the resistance to fluid invasion being replaced, respectively, by the magnetic field and the coercivity values h_i . Note that the invasion percolation process occurs without trapping. Indeed, and contrarily to the initially proposed case of two incompressible fluids, in a magnetic layer a trapped unreversed domain (i.e., an unreversed domain surrounded by a reversed domain) can be reversed if the magnetic field increases. Therefore, the generated percolating cluster is similar to those obtained in standard percolation. According to this simple analysis, the fact that both FePt/MgO and FePt/Pt layers possess very strong disorders is the reason why the observed domain patterns are similar at large scale.

Let us now focus on the effects of dipolar field. At smaller disorder strengths, the demagnetizing field becomes important. At small length scales one observes a dendritic pattern reminiscent of the serpentine observed in equilibrium configurations (see, e.g., Refs. 16 and 17). In order to reproduce our experimental results, where such demagnetizing field effects can be observed at low scales [cf. Figs. 2(a) and 2(b)], we had to determine the appropriate values of the parameters α/J and Δ/J . The first ratio can be extracted from experimental characteristics of our samples ($M_S = 1.03 \times 10^6\ \text{A m}^{-1}$, $K_U = 5.0 \times 10^6\ \text{J m}^3$, and $A = 6.9 \times 10^{-12}\ \text{J m}^{-1}$), using the modeling of thin films by an Ising model described in Ref. 15; we thus find $\alpha/J = 0.27$.

The pertinent value of the disorder strength Δ/J cannot be easily extracted from experimental characterization. We have therefore simulated the dynamics presented above for different values of this ratio. As expected, the short-distance properties are strongly influenced by the demagnetizing field. In Fig. 3 we show the typical short-distance behavior of the flipped domain. At $\Delta/J = 0.15$ the demagnetizing field is responsible for the dendritic behavior seen in Fig. 3(a). Self-avoidance of growing dendrites gives rise to a pattern similar

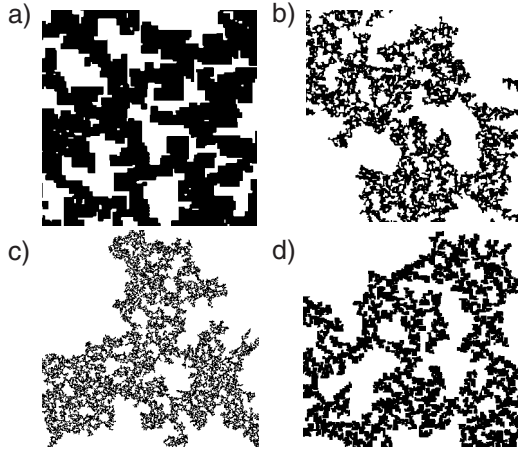


FIG. 3. Patterns observed at the percolation threshold using $\alpha/J=0.27$. The disorder strength is $\Delta/J=0.15$ for (a), (c) and $\Delta/J=0.8$ for (b), (d). (a) and (b) are 250 pixels large, and are magnified parts. (c) and (d), which are 1024 pixels large. A dendritic structure with typical size of around ten pixels is clearly seen in Fig. 3(a), reproducing qualitatively the experimental data [see Figs. 2(a) and 2(b)]. For a larger disorder [Fig. 3(b)] the structure is still fractal down to the size of the pixel. The obtained geometries are quantitatively and qualitatively similar at large distances to those obtained in the simple percolation problem [cf. Figs. 2(g) and 2(h)].

to that observed in experimental systems [see Figs. 2(a) and 2(b)]. At higher Δ/J the effect of demagnetizing field disappears and we retrieve the pattern observed in IPWT [see Fig. 3(b)], which is fractal down to the pixel.

Although the short-distance regime is clearly affected by the presence of the demagnetizing field, the long-distance properties are not modified by the long-range interaction. This can be seen in Figs. 3(c) and 3(d), where one observes that the fractal structures are qualitatively similar. The independence of the long-distance properties of the percolating cluster with respect to demagnetizing field can be made more quantitatively by analyzing the fractal dimension of the reversed cluster. In Fig. 4, we show the typical box-counting log-log plot, for systems with different strengths of disorder. The slope of the curve gives the fractal dimension, the linearity being linked to the self-similarity. The straight line which corresponds to the fractal dimension of a standard percolating cluster provides a good fit of the simulation results. These results suggest that the demagnetizing field (i.e., the dipolar interaction), even if strong enough to lead to a dendritic pattern at low scale, does not change in a significant way the critical properties of the percolating cluster. Using similar computations, we have also checked that a change in ratio α/J in a reasonable range does not modify significantly the critical properties of the percolating cluster.

According to the results obtained using the RFIM, the observed universality is thus due to the domination of disorder, and should not be modified by demagnetizing field effects. However, one can wonder whether this result is model dependent. Apart from Ising-type models, domain-growth models in magnetic thin layers with perpendicular magnetization are usually micromagnetic models,¹⁵ where the

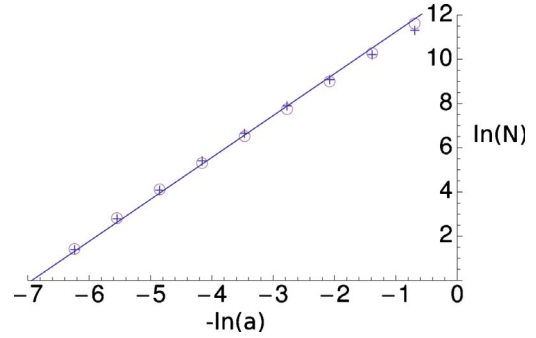


FIG. 4. (Color online) Log-log plot of the box-counting method: the sample is divided in boxes of size a (in arbitrary units), and N corresponds to the number of boxes in which there exists a returned spin. The crosses correspond to $\Delta/J=0.8$ and the open circles to $\Delta/J=0.15$. The plain curve is a line with a slope of $91/48$ that corresponds to the theoretical value for a percolation cluster and fits quite nicely the simulation results.

elementary cells composing the layers possess specific properties (anisotropy, volume,...), and which most often include a dipolar long-range interaction. Most of those cell models take basically into account the applied field, a disorder source (anisotropy fluctuations,...), an exchange-like interaction between cells and a dipolar interaction. Thus, they simply map to the RFIM model with dipolar interaction used in this study, and lead to similar results when looking for critical properties. Moreover, in the strong disorder limit, the dipolar interactions are negligible. In such case, the growth in any cell model can be summarized exactly like an IPWT problem: the applied field determines simply the ratio of cell which can be reversed, and a cell can be reversed if and only if an adjacent cell is already reversed. Therefore, the only ingredients necessary to obtain a percolation-like pattern are the existence of two states of magnetization, and the presence of a disorder strong enough to pin efficiently the layer. The results obtained in this study may consequently be generalized to 2D magnets reversed by domain-wall propagation, as long as they possess a strong disorder: especially, similar geometries of magnetic domains should be observed at large scale, especially in similar magnetic layers with perpendicular anisotropy (CoPt, CoNi,...).

Still, some conditions are required to observe such geometries. Experimentally, a large density of nucleation centers can prevent the observation of self-similarity, the mean distance between centers being an upper limit for the scale invariance. Indeed, depending on the characteristic lengths of the problem (domain-wall width, equilibrium domain size), the mean distance between nucleation centers can be smaller than the equilibrium domain size, above which the geometry is supposed to be fractal. Also, if the applied field is much bigger than the coercive field, the domain wall can detach itself from all pinning centers, and the growth pattern should then be controlled by dynamical KPZ-type equations.

To sum it up, the similarity of the large-scale geometries of the reversed domain in FePt/Pt and FePt/MgO layers can be understood on the basis of standard domain-growth models (IPWT, RFIM at zero temperature, cell models). It thus provides an original example of criticality-related universal-

ity, which can be transposed to other magnetic thin layers. Our simulations based on the RFIM suggest that the introduction of demagnetizing field does not modify the universality class. An interesting development of this work might

be to use fields largely higher than the coercive field, to study the transition between 2D percolationlike growth and $1+1$ D growth, which is then expected to be in the universality class of the one-dimensional KPZ equation.

*jean-philippe.attane@cea.fr

- ¹M. Kardar, G. Parisi, and Y.-C. Zhang, *Phys. Rev. Lett.* **56**, 889 (1986).
- ²S. F. Edwards and D. R. Wilkinson, *Proc. R. Soc. London, Ser. A* **381**, 17 (1982).
- ³M. Jost, J. Heimele, and T. Kleinefeld, *Phys. Rev. B* **57**, 5316 (1998).
- ⁴L. Miettinen, M. Mylly, J. Merikoski, and J. Timonen, *Eur. Phys. J. B* **46**, 55 (2005).
- ⁵M. P. M. den Nijs, *J. Phys. A* **12**, 1857 (1979).
- ⁶A. Bunde and S. Havlin, *Fractal and Disordered Systems* (Springer-Verlag, Berlin, 1991), Chap. 2.
- ⁷H. Ji and M. O. Robbins, *Phys. Rev. A* **44**, 2538 (1991).
- ⁸H. Ji and M. O. Robbins, *Phys. Rev. B* **46**, 14519 (1992).
- ⁹D. Wilkinson and J. Willemsen, *J. Phys. A* **16**, 3365 (1983).
- ¹⁰J. P. Attané, Y. Samson, A. Marty, D. Halley, and C. Beigné, *Appl. Phys. Lett.* **79**, 794 (2001).
- ¹¹J. P. Attané, Y. Samson, A. Marty, J. C. Toussaint, G. Dubois, A. Mougin, and J. P. Jamet, *Phys. Rev. Lett.* **93**, 257203 (2004).
- ¹²D. Halley, Y. Samson, A. Marty, P. Bayle-Guillemaud, C. Beigné, B. Gilles, and J. E. Mazille, *Phys. Rev. B* **65**, 205408 (2002).
- ¹³T. Jourdan, J. P. Attané, F. Lançon, C. Beigné, L. Vila, and A. Marty, *J. Magn. Magn. Mater.* **321**, 2187 (2009).
- ¹⁴K. Foroutan-pour, P. Dutilleul, and D. L. Smith, *Appl. Math. Comput.* **105**, 195 (1999).
- ¹⁵A. Lyberatos, *J. Phys. D* **33**, R117 (2000).
- ¹⁶L. C. Sampaio, M. P. de Albuquerque, and F. S. de Menezes, *Phys. Rev. B* **54**, 6465 (1996).
- ¹⁷A. B. MacIsaac, J. P. Whitehead, M. C. Robinson, and K. De'Bell, *Phys. Rev. B* **51**, 16033 (1995).